

Distributed PI Formation Control Design for Autonomous Vehicles Using Edge Dynamics

Dinh Hoa Nguyen

*International Institute for Carbon-Neutral Energy Research,
and the Institute of Mathematics for Industry,
Kyushu University, Fukuoka 819-0395, Japan.
(e-mail: hoa.nd@i2cner.kyushu-u.ac.jp)*

Abstract: A novel fully distributed proportional-integral (PI) formation controller design approach is proposed in this paper for general linear multi-agent systems (MASs) with model uncertainties and disturbances. First, an edge dynamics is developed for uncertain and perturbed linear MASs, based on which the formation control problem for the initial MAS is shown to be equivalent to a decentralized stabilizing problem for the obtained edge dynamics. Afterward, a necessary and sufficient condition for the PI controller gains is derived. A corollary of this condition shows that for integrator agents, PI controller gains can be any positive scalars. This result is then applied to the formation control of autonomous four-wheel vehicles described by nonlinear models, of which the efficiency of the proposed method is demonstrated in presence of both uncertainties and disturbances.

Keywords: Edge Dynamics, Multi-Agent System, Networked Systems, Formation Control, Disturbance Rejection, Distributed PI Controller, Uncertainty, Autonomous Vehicles.

1. INTRODUCTION

Multi-agent system (MAS) and its cooperative control problems are very attractive for many research disciplines since a lot of practical problems, e.g. those in robotics, power grids, transportation networks, mechanical engineering, systems biology, aerospace engineering, etc., can be formulated and studied using MAS control theory. One key property of MASs is the ability to achieve global goals for the whole MAS system by utilizing only local measurement and control at each agent and the sparse information exchange between agents.

Formation control is an important and extensively investigated direction for MASs, which is originated from observed motions in nature and then has been applied to many real-life and engineering systems, see e.g., Olfati-Saber et al. (2007); Ren et al. (2007). In particular, formation control of autonomous (unmanned) vehicles and robots, which can be on ground, in space, on water surface, or underwater, has gained much interest from both academic and industrial communities. Some recent surveys of such MAS formation can be found in Oh et al. (2015); Soni and Hu (2017); Hu et al. (2017).

In the current research, the synthesis of fully distributed formation controllers for MASs subject to model uncertainties and disturbances is studied. In the literature, there have been several studies on this problem, e.g., using H_∞ and integral backstepping method W. Jasim and D. Gu (2018), LQR-based approaches H. Liu and T. Ma and F. L. Lewis and Y. Wan (2019); Y. Hua and X. Dong and Q.

Li and Z. Ren (2017), nonlinear designs X. Wang and X. Fan (2019); X. Ai and J. Yu (2019).

Note that in order to obtain fully distributed formation controllers for MASs using only local information, the relative information between agents must be employed. In other words, the information on the edges of inter-agent communication graph is essential. Moreover, an MAS formation is formally defined as a set of desired inter-agent states or outputs. Therefore, the inter-agent (i.e., edge) dynamic responses are very important for the MAS formation control, in addition to individual dynamics of each agent. This leads to a recent research direction on edge dynamics for MASs, see e.g., D. Zelazo and M. Mesbahi (2011); D. Zelazo and S. Schuler and F. Allgower (2013); D. Mukherjee and D. Zelazo (2018), Z. Zeng and X. Wang and Z. Zheng (2016), Nguyen (2017); Nguyen et al. (2018), leader-follower nonlinear MASs N. R. Chowdhury and S. Sukumar and M. Maghenem and A. Loria (2018).

In our previous works Nguyen (2017); Nguyen et al. (2018), edge dynamics was introduced for consensus control problems. It should be emphasized that although consensus is closely related to formation, an edge dynamics for MAS formation with general dynamics of agents is not straightforwardly obtained from that for MAS consensus. Furthermore, disturbances were not considered in Nguyen (2017); Nguyen et al. (2018), and only static controllers were introduced there. On the other hand, the current research investigates general linear dynamics of agents with model uncertainties and disturbances. Accordingly, a fully distributed dynamic PI controller is proposed here to handle such uncertainties and disturbances. Moreover,

a necessary and sufficient condition is derived for the designed PI controller to achieve the desired formation for the considering MAS. To the best of author's knowledge, such a design and its related results have not been introduced in the literature so far.

The rest of this paper is organized as follows. Section 2 presents the uncertain and perturbed MAS model and then the edge dynamics for the distributed formation control problem, which are then followed by the proposed fully distributed PI controller design. Next, in Section 3 the model of autonomous ground vehicles and its coordinate transformation are given. Consequently, the application of the proposed PI formation control design for autonomous vehicle groups together with simulation results for two scenarios are provided and compared in Section 4. Finally, the conclusion is given in Section 5.

The following notations and symbols will be used in the paper. \mathbb{R} and \mathbb{C} stand for the real and complex sets. \mathbb{R}^n , \mathbb{R}_+^n and \mathbb{C}^n are used to denote the set of real, positive real and complex $n \times 1$ vectors. Moreover, $\mathbf{1}_n$ and $\mathbf{0}_n$ denote the $n \times 1$ vector with all elements equal to 1 and 0, respectively; and I_n denotes the $n \times n$ identity matrix. Finally, \otimes stands for the Kronecker product

2. MAS FORMATION CONTROL

2.1 Communication Graph

The communication structure in the considering MAS is represented by an undirected graph \mathcal{G} with vertex set \mathcal{V} and edge set \mathcal{E} in which each vertex represents a robot and each edge $(k, j) \in \mathcal{E}$ corresponds to the interconnection between robots k and j . The neighboring set of robot k is denoted by $\mathcal{N}_k \triangleq \{j \in \mathcal{V} : (k, j) \in \mathcal{E}\}$. Moreover, let a_{kj} be elements of the adjacency matrix \mathcal{A} of \mathcal{G} , i.e. $a_{kj} = 1$ if $(k, j) \in \mathcal{E}$ and $a_{kj} = 0$ if $(k, j) \notin \mathcal{E}$. Then the degree matrix of \mathcal{G} is denoted by $\mathcal{D} = \text{diag}\{d_k\}_{k=1, \dots, n}$, where $d_k \triangleq \sum_{j \in \mathcal{N}_k} a_{kj}$. Consequently, the Laplacian matrix \mathcal{L} associated to \mathcal{G} is defined by $L = \mathcal{D} - \mathcal{A}$. Denote $E \in \mathbb{R}^{N \times M}$ an incidence matrix of \mathcal{G} where $M = |\mathcal{E}|$, then $L = EE^T$ and $E^T \mathbf{1}_N = 0$. Moreover, L^\dagger denotes the generalized pseudoinverse of L Gutman and Xiao (2004).

2.2 Edge Dynamics

Consider an uncertain MAS composing of N identical agents whose mathematical model is described by

$$\dot{x}_i(t) = (A + \Delta A)x_i(t) + (B + \Delta B)u_i(t) + B_d \xi_i(t), \quad (1)$$

where $A \in \mathbb{R}^{n \times n}$, $B \in \mathbb{R}^{n \times m}$, $B_d \in \mathbb{R}^{n \times p}$; $x_i(t) \in \mathbb{R}^n$ and $u_i(t) \in \mathbb{R}^m$ are the state and input vectors of the i th agent, respectively; $\xi_i(t) \in \mathbb{R}^p$ is a bounded disturbance; ΔA and ΔB are the bounded uncertainties on system matrices whose bounds are known. The whole MAS dynamics then can be represented by

$$\dot{\hat{x}}(t) = [I_N \otimes (A + \Delta A)]x(t) + [I_N \otimes (B + \Delta B)]u(t) + (I_N \otimes B_d)\xi(t), \quad (2)$$

where

$$\begin{aligned} x(t) &= [x_1(t)^T, \dots, x_N(t)^T]^T, \\ u(t) &= [u_1(t)^T, \dots, u_N(t)^T]^T, \\ \xi(t) &= [\xi_1(t)^T, \dots, \xi_N(t)^T]^T. \end{aligned}$$

The aim of controlling this MAS is to converge to a given formation pattern in spite of the existence of system uncertainties and disturbances, as defined below.

Definition 1. The MAS system (2) is said to reach a formation if the following condition is satisfied,

$$\lim_{t \rightarrow +\infty} [x_i(t) - x_j(t)] = x_{ij}^* \quad \forall i, j = 1, \dots, N, \quad (3)$$

where x_{ij}^* are constant vectors representing the desired formation pattern.

Note here that x_{ij}^* are the desired relative states of agents. Thus, we will not control agents to some fixed, known reference state for each of them, but to some states where their differences are as expected, and the absolute measurements are not needed for agents.

The following assumptions are made.

A1: $\sigma(A) \in \mathbb{C}_-$, and at least one eigenvalue of A is on the imaginary axis.

A2: (A, B) is controllable.

The purpose of assumption **A1** is to avoid the convergence of agents to infinity or zero Xiao and Wang (2007) whereas assumption **A2** is for the existence of a controller. Define new vectors

$$z \triangleq (E^T \otimes I_n)x, \quad w \triangleq (E^T \otimes I_m)u, \quad d \triangleq (E^T \otimes I_p)\xi,$$

then it can be shown, in a similar manner as that in Nguyen (2017), that the initial MAS becomes

$$\begin{aligned} \dot{z} &= [(E^T L^\dagger E) \otimes (A + \Delta A)]z + [I_M \otimes (A + \Delta A)]w \\ &\quad + (I_M \otimes B_d)d. \end{aligned} \quad (4)$$

We call (4) the uncertain and perturbed edge dynamics. The edge dynamics is important for studying formation control problems of MASs because it fully captures the difference on states of connected agents, and therefore the desired formation is obtained if and only if

$$\lim_{t \rightarrow +\infty} z(t) = z^*, \quad (5)$$

where $z^* \in \mathbb{R}^{Mn}$ is the vector of appropriate x_{ij}^* in (3). *This means the formation control problem now becomes a reference tracking problem for the edge dynamics (4).*

Let $\bar{L} = E^T L^\dagger E$ and $L_e = E^T E$. The algebraic properties of \bar{L} and L_e are given in the following lemma provided in Nguyen (2017).

Lemma 1. If \mathcal{G} is connected, then

- (i) L_e has exactly $N - 1$ non-zero eigenvalues, which are equal to positive eigenvalues of L while all other eigenvalues of L_e if exist are 0,
- (ii) \bar{L} has exactly $N - 1$ non-zero eigenvalues, which are all equal to 1, and other eigenvalues of \bar{L} if exists are 0.

Denote the edge tracking error by $\zeta \triangleq z - z^*$. The edge tracking error dynamics is

$$\begin{aligned} \dot{\zeta} &= [\bar{L} \otimes (A + \Delta A)]\zeta + [\bar{L} \otimes (A + \Delta A)]z^* \\ &\quad + [I_M \otimes (B + \Delta B)]w + (I_M \otimes B_d)d. \end{aligned} \quad (6)$$

Next, let $U \in \mathbb{R}^{M \times M}$ be an orthogonal matrix that diagonalizes \bar{L} , and

$$\check{\zeta} \triangleq (U^T \otimes I_n)\zeta, \quad \tilde{w} \triangleq (U^T \otimes I_m)w, \quad \tilde{d} \triangleq (U^T \otimes I_p)d.$$

Consequently, multiplying both sides of (6) with $U^T \otimes I_n$ gives us

$$\begin{aligned} \dot{\zeta} &= [\bar{\Gamma} \otimes (A + \Delta A)] \tilde{\zeta} + [\bar{\Gamma} \otimes (A + \Delta A)] \tilde{z}^* \\ &\quad + [I_M \otimes (B + \Delta B)] \tilde{w} + (I_M \otimes B_d) \tilde{d}, \end{aligned} \quad (7)$$

where $\bar{\Gamma} \triangleq \text{diag}\{0, I_{N-1}\}$ and $\tilde{z}^* \triangleq (U^T \otimes I_n) z^*$. Partitioning U , $\tilde{\zeta}$, \tilde{z}^* , and \tilde{w} as follows,

$$U = [U_1 \ U_2], \tilde{\zeta} = \begin{bmatrix} \tilde{\zeta}_1 \\ \tilde{\zeta}_2 \end{bmatrix}, \tilde{z}^* = \begin{bmatrix} \tilde{z}_1^* \\ \tilde{z}_2^* \end{bmatrix}, \tilde{w} = \begin{bmatrix} \tilde{w}_1 \\ \tilde{w}_2 \end{bmatrix}, \tilde{d} = \begin{bmatrix} \tilde{d}_1 \\ \tilde{d}_2 \end{bmatrix},$$

where

$$\begin{aligned} U_1 &\in \mathbb{R}^{M \times (M-N+1)}, \quad U_2 \in \mathbb{R}^{M \times (N-1)}, \\ \tilde{\zeta}_1 &\in \mathbb{R}^{n(M-N+1)}, \quad \tilde{\zeta}_2 \in \mathbb{R}^{n(N-1)}, \\ \tilde{z}_1^* &\in \mathbb{R}^{n(M-N+1)}, \quad \tilde{z}_2^* \in \mathbb{R}^{n(N-1)}, \\ \tilde{w}_1 &\in \mathbb{R}^{m(M-N+1)}, \quad \tilde{w}_2 \in \mathbb{R}^{m(N-1)}, \\ \tilde{d}_1 &\in \mathbb{R}^{p(M-N+1)}, \quad \tilde{d}_2 \in \mathbb{R}^{p(N-1)}. \end{aligned}$$

Then

$$\begin{aligned} \tilde{\zeta}_1 &= (U_1^T \otimes I_n) \zeta, \quad \tilde{\zeta}_2 = (U_2^T \otimes I_n) \zeta, \\ \tilde{w}_1 &= (U_1^T \otimes I_m) w, \quad \tilde{w}_2 = (U_2^T \otimes I_m) w, \\ \tilde{d}_1 &= (U_1^T \otimes I_p) d, \quad \tilde{d}_2 = (U_2^T \otimes I_p) d, \end{aligned}$$

and (7) is equivalent to

$$\begin{aligned} \dot{\tilde{\zeta}}_1 &= [I_{M-N+1} \otimes (B + \Delta B)] \tilde{w}_1 + (I_{M-N+1} \otimes B_d) \tilde{d}_1, \\ \dot{\tilde{\zeta}}_2 &= [I_{N-1} \otimes (A + \Delta A)] \tilde{\zeta}_2 + [I_{N-1} \otimes (A + \Delta A)] \tilde{z}_2^* \\ &\quad + [I_{N-1} \otimes (B + \Delta B)] \tilde{w}_2 + (I_{N-1} \otimes B_d) \tilde{d}_2. \end{aligned} \quad (8)$$

Equation (8) is called the decomposed edge dynamics for the considered uncertain and perturbed MAS.

2.3 Distributed PI Formation Control Synthesis

It can be seen from (8) that the edge dynamics is now decomposed into two decentralized subsystems. We will prove in Lemma 2 that the first subsystem is always at the origin, hence we only need to design the control input for the second subsystem. Further, the design of control input \tilde{w}_2 is decentralized since the second subsystem is decentralized and the communication structure among agents is already implicitly embedded in $\tilde{\zeta}_2$ and \tilde{w}_2 through matrix U .

Lemma 2. The state $\tilde{\zeta}_1(t)$, control input $\tilde{w}_1(t)$, and disturbance $\tilde{d}_1(t)$ are always equal to 0 for all $t \geq 0$.

Proof. Indeed, we have $\tilde{\zeta}_1 = U_1^T \zeta = [(U_1^T E^T) \otimes I_n](x - x^*)$, where $x^* \in \mathbb{R}^{Nn}$ such that $(E^T \otimes I_n)x^* = z^*$. Next, $EU_1 = E\bar{L}U_1$, because $E\bar{L} = EE^T L^\dagger E = LL^\dagger E = E$. On the other hand, $\bar{L}U_1 = U_1^T U^T U_1 = 0$. Therefore, $EU_1 = 0$. This leads to $\tilde{\zeta}_1(t) = 0 \forall t \geq 0$. Similarly, we can show that $\tilde{w}_1(t)$ and $\tilde{d}_1(t)$ are equal to 0 for all $t \geq 0$. \square

Now, the remaining problem is to design a decentralized stabilizing controller $\tilde{w}_2(t)$ to make $\tilde{\zeta}_2(t) \rightarrow 0$ despite the existence of the uncertainties $\Delta A, \Delta B$, and the disturbance $\tilde{d}_2(t)$. In this paper, we introduce such a synthesis when the disturbance $\tilde{d}_2(t)$ is in form of a step signal.

Define a new state variable $\eta \in \mathbb{R}^{nM}$ that

$$\dot{\eta} = \tilde{\zeta}, \quad \eta(0) = 0.$$

Accordingly, we also define η_1 and η_2 such that

$$\eta = [\eta_1^T \ \eta_2^T]^T, \quad \eta_1 \in \mathbb{R}^{n(M-N+1)}, \quad \eta_2 \in \mathbb{R}^{n(N-1)}.$$

With these new variables, (8) can be restated as follows,

$$\begin{aligned} \dot{\eta}_2 &= \tilde{\zeta}_2, \\ \dot{\tilde{\zeta}}_2 &= [I_{N-1} \otimes (A + \Delta A)] \tilde{\zeta}_2 + [I_{N-1} \otimes (A + \Delta A)] \tilde{z}_2^* \\ &\quad + [I_{N-1} \otimes (B + \Delta B)] \tilde{w}_2 + (I_{N-1} \otimes B_d) \tilde{d}_2. \end{aligned} \quad (9)$$

Let $\Gamma \in \mathbb{R}^{(N-1) \times (N-1)}$ be the diagonal matrix including all non-zero eigenvalues of L in its diagonal, and $V \in \mathbb{R}^{N \times N}$ be an orthogonal matrix such that

$$V^T L V = \begin{bmatrix} 0 & 0 \\ 0 & \Gamma \end{bmatrix}. \quad (10)$$

Partitioning V into $[V_1, V_2]$ where $V_1 \in \mathbb{R}^N$, $V_2 \in \mathbb{R}^{N \times (N-1)}$. Then

$$L V_2 = V_2 \Gamma \Leftrightarrow V_2^T L V_2 = \Gamma, \quad (11)$$

since $V_2^T V_2 = I_{N-1}$. The following theorem shows the equivalence of a decentralized stabilizing controller for the edge dynamics to a distributed formation controller for the initial MAS, and an associated condition for controller gains.

Theorem 3. Given a connected communication graph \mathcal{G} , choose U_2 to be $E^T V_2 \Gamma^{-1/2}$, the following decentralized PI controller is proposed for (8),

$$\tilde{w}_2(t) = -(\Gamma \otimes K_P) \tilde{\zeta}_2(t) - (\Gamma \otimes K_I) \eta_2(t), \quad (12)$$

which is equivalent to the decentralized PI controller

$$\tilde{w} = - \begin{bmatrix} 0 & 0 \\ 0 & \Gamma \otimes K_P \end{bmatrix} \tilde{\zeta} - \begin{bmatrix} 0 & 0 \\ 0 & \Gamma \otimes K_I \end{bmatrix} \eta, \quad (13)$$

for the transformed edge dynamics (7) and the following fully distributed PI controller for the initial MAS (2),

$$\begin{aligned} u_i(t) &= -K_P \sum_{j \in \mathcal{N}_i} (x_i(t) - x_j(t) - x_{ij}^*) \\ &\quad - K_I \sum_{j \in \mathcal{N}_i} \int_0^t (x_i(\tau) - x_j(\tau) - x_{ij}^*) d\tau, \end{aligned} \quad (14)$$

or equivalently the following controller,

$$u(t) = -(L \otimes K_P)(x(t) - x^*) - (L \otimes K_I) \int_0^t (x(\tau) - x^*) d\tau. \quad (15)$$

Further, (13) is a decentralized PI *stabilizing* controller, and equivalently, (14) is a distributed PI *formation* controller, if and only if all eigenvalues of the following characteristic equations belong to the closed left half complex plane,

$$s^2 I_n - s[A + \Delta A - \lambda_i(B + \Delta B)K_P] + \lambda_i(B + \Delta B)K_I \quad (16)$$

for all $i = 2, \dots, N$.

Proof. The equivalence of controllers (13) and (12) can be easily obtained using $\tilde{\zeta}_1(t) = 0$, $\tilde{w}_1(t) = 0$, and $\tilde{d}_1(t) = 0$ stated in Lemma 2. On the other hand, the equivalence between the two controllers (13) and (14) follows the proof in Nguyen (2017) and is skipped here for brevity.

Next, we show that (13) stabilizes the transformed edge dynamics (7), which also means that (14) makes the MAS achieving the desired formation, if and only if (16) is satisfied. It is then enough to show that (13) stabilizes (8) as long as (16) is satisfied. Indeed, substituting (13) back to (9) gives us the following closed-loop state space equation,

$$\begin{bmatrix} \dot{\eta}_2 \\ \dot{\tilde{\zeta}}_2 \end{bmatrix} = \mathbb{A} \begin{bmatrix} \eta_2 \\ \tilde{\zeta}_2 \end{bmatrix} + \begin{bmatrix} 0 \\ I_{N-1} \otimes [(A + \Delta A)\tilde{z}_2^* + B_d \tilde{d}_2] \end{bmatrix}, \quad (17)$$

where \mathbb{A} is defined by

$$\begin{bmatrix} 0 & I_{n(N-1)} \\ -\Gamma \otimes [(B + \Delta B)K_I] & I_{N-1} \otimes (A + \Delta A) - \Gamma \otimes [(B + \Delta B)K_P] \end{bmatrix}.$$

It can be easily seen that the linear system in (17) has an equilibrium point if and only if all eigenvalues of \mathbb{A} lie on the closed left half complex plane. Further, the equilibrium point of (17) is $(\eta_2^{eq}, 0)$, where η_2^{eq} is the solution of the equation

$$-(\Gamma \otimes [(B + \Delta B)K_I])\eta_2^{eq} = I_{N-1} \otimes [(A + \Delta A)\tilde{z}_2^* + B_d\tilde{d}_2].$$

That means $\tilde{\zeta}_2$ is stabilized by the decentralized PI controller (12) if and only if \mathbb{A} is not unstable.

All eigenvalues of \mathbb{A} can be found by solving the characteristic equation $\det(sI - \mathbb{A}) = 0$. Using a property of the determinant for block square matrices, we can easily show that

$$\det(sI - \mathbb{A}) = \prod_{i=2}^N \det(s^2 I_n - s[A + \Delta A - \lambda_i(B + \Delta B)K_P] + \lambda_i(B + \Delta B)K_I). \quad (18)$$

Hence, all eigenvalues of \mathbb{A} are the roots of characteristic equations (16). This concludes the proof. \square

Theorem 3 shows the synthesis of distributed PI formation controllers for MASs with general linear dynamics of agents. For a particular case when the dynamics of agents is just an integrator, the following corollary reveals a more specific and explicit result by directly checking the roots of the polynomials $s^2 I_n - s[A + \Delta A - \lambda_i(B + \Delta B)K_P] + \lambda_i(B + \Delta B)K_I$ for all $i = 2, \dots, N$.

Corollary 2.1. When agents' dynamics is an uncertain integrator, i.e., $A = 0$, $B = 1$, $\Delta A = 0$, $\Delta B > -1$, (14) is a distributed PI formation controller for any $K_P > 0$ and any $K_I > 0$.

3. UNMANNED VEHICLE MODEL

In the current research, a more complex model than double-integrator of unmanned vehicles with front-wheel steering is studied. First, the nonlinear model of vehicles is transformed to a new model of a set of integrators in a new coordinate. Next, the distributed PI formation controller synthesis for integrator MASs will be utilized for that transformed model, subjected to model uncertainties and disturbances.

The variables and parameters of each vehicle are illustrated in Figure 1 where the center of mass is denoted by M_i whose position in a global coordinate frame (O, x, y) is represented by (x_{M_i}, y_{M_i}) . The rotation and steering angles are denoted by θ_i and φ_i , respectively. Accordingly, ω_i and v_i represent the angular and longitudinal velocity. Then the mathematical model of 4-wheel robots with front-wheel steering, $i = 1, \dots, N$, is represented by

$$\begin{aligned} \dot{\theta}_i &= \omega_i = v_i \tan \varphi_i, \\ \dot{x}_{M_i} &= v_i \cos \theta_i, \\ \dot{y}_{M_i} &= v_i \sin \theta_i. \end{aligned} \quad (19)$$

In this model, the control inputs for each robot are the steering angle φ_i and the longitudinal speed v_i , where the rotation angles θ_i are assumed to be measurable. However, to capture the real situations, we here study the system

with inexact measurement of the rotation angles, i.e., $\theta_i = \theta_i^0 + \Delta\theta_i$, where $\Delta\theta_i$ represents the small inexactness or uncertainty in the measurement.

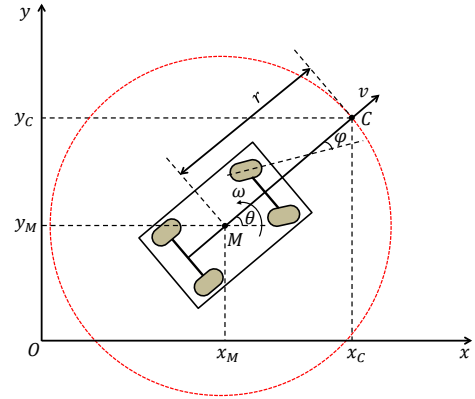


Fig. 1. Demonstration of variables defined for a 4-wheel vehicle.

Subsequently, the formation problem of this vehicle group is to find proper control inputs for vehicles such that they shall converge to a desired formation pattern, from any initial locations and any initial heading angles. The formation pattern can be assigned to the center of mass of vehicles. However, in reality we cannot treat vehicles as mass points. In addition, the collision avoidance should be taken into account for the vehicle group. Therefore, the formation pattern will be represented in terms of the vehicles' heading points $C_i, i = 1, \dots, N$, which are defined as follows. Let r be the radius of a circle centered at M_i which represents the safety region of the i th vehicle, i.e., to avoid the collision with other vehicles while they are moving. Then C_i is the intersection of the speed vector with that circle, as depicted in Figure 1.

Let us denote $\bar{x}_i \triangleq \begin{bmatrix} x_{C_i} \\ y_{C_i} \end{bmatrix}$ and $M_i \triangleq \begin{bmatrix} \cos \theta_i & -r \sin \theta_i \\ \sin \theta_i & r \cos \theta_i \end{bmatrix}$, then the vehicle's model can be rewritten in terms of the coordinates of C_i as follows,

$$\dot{\bar{x}}_i = M_i[v_i, \omega_i]^T, i = 1, \dots, N. \quad (20)$$

Note here that due to the uncertainty on the rotation angles measurement, M_i are now uncertain matrices with uncertain parameters $\Delta\theta_i$. Because we assume that those uncertain parameters are small, we can approximate

$$\sin \Delta\theta_i \approx 0, \quad \cos \Delta\theta_i \approx 1 + \frac{1}{2}\Delta\theta_i^2.$$

Therefore, $M_i \approx M_i^0 + \delta_i M_i^0$, where $\delta_i \triangleq \frac{1}{2}\Delta\theta_i^2$ and $M_i^0 \triangleq \begin{bmatrix} \cos \theta_i^0 & -r \sin \theta_i^0 \\ \sin \theta_i^0 & r \cos \theta_i^0 \end{bmatrix}$. Accordingly, (20) becomes

$$\dot{\bar{x}}_i = (M_i^0 + \delta_i M_i^0)[v_i, \omega_i]^T, i = 1, \dots, N, \quad (21)$$

Denote

$$\bar{u}_i \triangleq M_i^0[v_i, \omega_i]^T,$$

then each vehicle can be represented by a set of two integrators as follows,

$$\dot{\bar{x}}_i = (1 + \delta_i)\bar{u}_i, i = 1, \dots, N. \quad (22)$$

Subsequently, we will compute

$$\begin{bmatrix} v_i \\ \omega_i \end{bmatrix} = M_i^{-1}\bar{u}_i = \begin{bmatrix} \cos \theta_i & \sin \theta_i \\ -\sin \theta_i/r & \cos \theta_i/r \end{bmatrix} \bar{u}_i \triangleq \begin{bmatrix} \tilde{u}_{i,1} \\ \tilde{u}_{i,2} \end{bmatrix}. \quad (23)$$

Therefore, the real control inputs v_i and φ_i to the vehicle are calculated by

$$v_i = \tilde{u}_{i,1}, \quad \varphi_i = \arctan \frac{\omega_i}{v_i} = \arctan \frac{\tilde{u}_{i,2}}{\tilde{u}_{i,1}}. \quad (24)$$

In summary, the control inputs \tilde{u}_i will be synthesized followed the proposed design in Section 2, then the longitudinal and rotational speeds v_i and ω_i are calculated by (23). Afterward, the actual control inputs fed to vehicles are computed by (24).

4. SIMULATION FOR PI FORMATION CONTROL OF AN UNMANNED GROUND VEHICLE GROUP

In this section, the efficiency of the proposed formation control design based on the edge dynamics is illustrated. For clarity, a group of only three unmanned vehicles is employed. The desired formation pattern is a triangle which is represented by the relative positions of vehicles in a global coordinate as follows,

$$\bar{x}_1 - \bar{x}_2 = [-4 \ -2]^T, \bar{x}_2 - \bar{x}_3 = [2 \ -2]^T, \bar{x}_3 - \bar{x}_1 = [2 \ 4]^T.$$

The initial positions of three vehicles are randomly chosen, while the initial heading angles in the global coordinate are selected to be different as follows,

$$\theta_1(0) = \frac{\pi}{4}, \theta_2(0) = \frac{-\pi}{3}, \theta_3(0) = \frac{2\pi}{3}.$$

4.1 With input disturbance

Assume that there are disturbances to vehicles represented by step inputs to the model (22). The step time is at 3, 5, and 7 seconds for vehicle 1, 2, and 3; and the step magnitude is 2, 1, and 1 for vehicle 1, 2, and 3; respectively. Then the proposed controller design, particularly Corollary 1, states that PI controller gains can be any positive numbers. Hence, we choose $K_P = 0.1$ and $K_I = 0.1$.

The simulation results are then exhibited in Figures 2–4. As seen from Figure 2, the considering unmanned vehicle group eventually reaches the desired formation shape, which can also be verified from Figure 3 where the relative positions of vehicles come to the desired values. Vehicles' rotating angles are displayed in Figure 4.

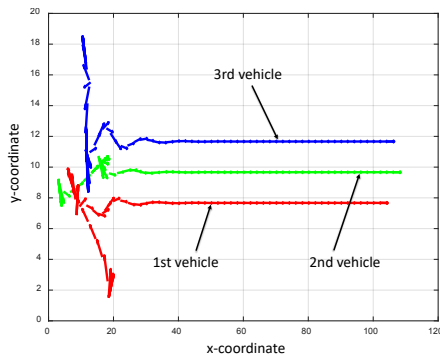


Fig. 2. Trajectories of vehicles under input disturbances.

4.2 With input disturbance and rotation angle uncertainty

The input disturbances are the same as in the previous section, while the uncertainty on rotation angle measurement is 0.5, 0.3, and -0.2 [rad] for vehicle 1, 2, and 3.

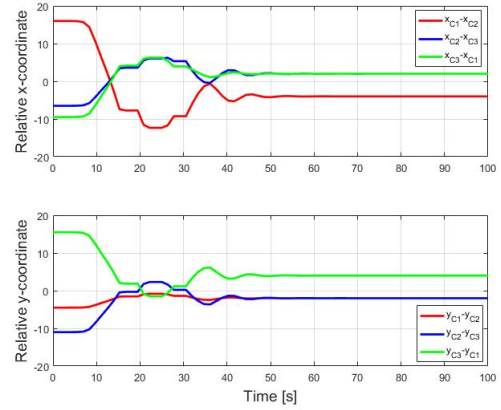


Fig. 3. Convergence of vehicles' relative positions under input disturbances.

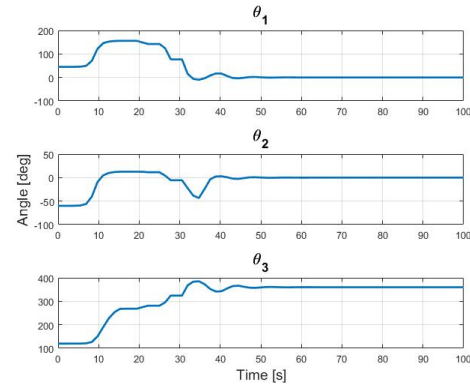


Fig. 4. Convergence of vehicles' rotating angles under input disturbances.

Then the simulation results are exhibited in Figures 5–7. Compared to the results when no rotation angle uncertainties exist, the responses of vehicles are obviously not the same and take longer time for achieving formation. Particularly, the trajectories of vehicles in Fig. 5 are very different due to the measurement uncertainties on rotation angles of vehicles, though the desired formation is still achieved. Moreover, Figures 6–7 reveal that oscillatory transient responses exist, and the rotation angle responses of vehicle 1 and 2 are completely different from those in the scenario that no rotation angle uncertainties are presented.

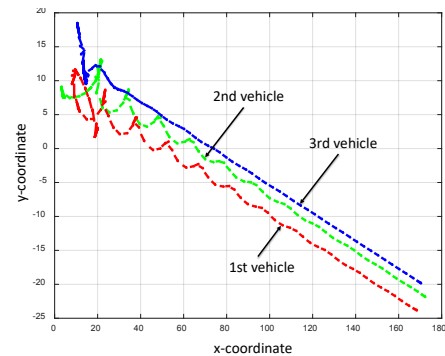


Fig. 5. Trajectories of vehicles under input disturbances and rotation angle uncertainties.

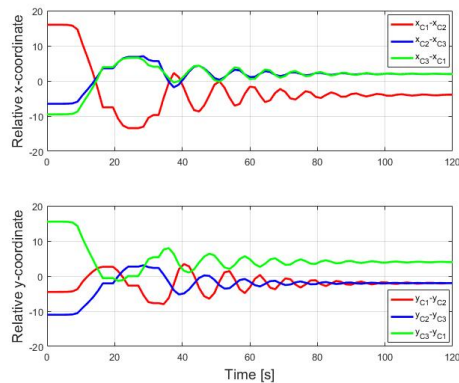


Fig. 6. Convergence of vehicles' relative positions under input disturbances and uncertainty of rotation angles.

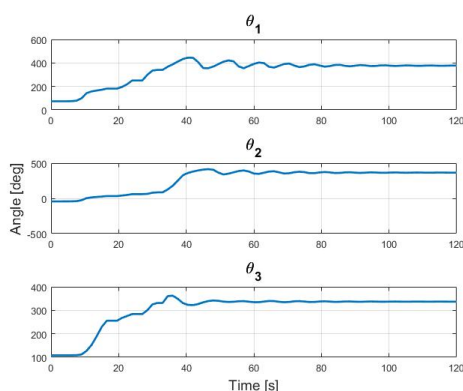


Fig. 7. Convergence of vehicles' rotating angles under input disturbances and uncertainty of rotation angles.

5. CONCLUSION

In this paper, a novel fully distributed PI formation controller design method is proposed for general linear MASs with model uncertainties and disturbances. By employing the edge dynamics, the formation control design is transformed into a stabilizing problem which is much easier to handle than the manifold convergence problem for the initial MAS. Then a necessary and sufficient stability condition is derived for the PI controller gains so that the formation can be achieved. The efficiency of the proposed design is then verified by its application to the formation control of autonomous vehicle groups, where the model uncertainties and disturbances exist but the desired formation is still achieved.

The future research will deal with several additional issues such as communication delays, directed communication graphs, etc.

REFERENCES

D. Mukherjee and D. Zelazo (2018). Robustness of Consensus over Weighted Digraph. *IEEE Transactions on Network Science and Engineering*, PP, 1–14.

D. Zelazo and M. Mesbahi (2011). Edge agreement: Graph-theoretic performance bounds and passivity analysis. *IEEE Transactions on Automatic Control*, 56(3), 544–555.

D. Zelazo and S. Schuler and F. Allgower (2013). Performance and design of cycles in consensus networks. *Systems and Control Letters*, 62(1), 85–96.

Gutman, I. and Xiao, W. (2004). Generalized inverse of the laplacian matrix and some applications. *Bulletin Classe des Sciences Mathematiques et Naturelles, Sciences mathematiques*, 129(29), 15–723.

H. Liu and T. Ma and F. L. Lewis and Y. Wan (2019). Robust Formation Trajectory Tracking Control for Multiple Quadrotors With Communication Delays. *IEEE Transactions on Control Systems Technology*, PP, 1–8.

Hu, Z., Wang, W., Zhang, G., and Han, C. (2017). A survey on the formation control of multiple quadrotors. In *Proc. of 2017 14th International Conference on Ubiquitous Robots and Ambient Intelligence (URAI)*, 219–225.

N. R. Chowdhury and S. Sukumar and M. Maghenem and A. Loria (2018). On the estimation of algebraic connectivity in graphs with persistently exciting interconnections. *International Journal of Control*, 91(1), 131–144.

Nguyen, D.H. (2017). Reduced-order distributed consensus controller design via edge dynamics. *IEEE Transactions on Automatic Control*, 62(1), 475–480.

Nguyen, D.H., Narikiyo, T., and Kawanishi, M. (2018). Robust consensus analysis and design under relative state constraints or uncertainties. *IEEE Transactions on Automatic Control*, 63(6), 1694–1700.

Oh, K.K., M-C.Park, and Ahn, H.S. (2015). A survey of multi-agent formation control. *Automatica*, 53, 424–440.

Olfati-Saber, R., Fax, J.A., and Murray, R.M. (2007). Consensus and cooperation in networked multi-agent systems. *Proc. IEEE*, 95(1), 215–233.

Ren, W., Beard, R.W., and Atkins, E.M. (2007). Information consensus in multivehicle cooperative control. 27(2), 71–82.

Soni, A. and Hu, H. (2017). Formation Control for a Fleet of Autonomous Ground Vehicles: A Survey. *Robotics*, 7(17), 1–25.

W. Jasim and D. Gu (2018). Robust Team Formation Control for Quadrotors. *IEEE Transactions on Control Systems Technology*, 26(4), 1516–1523.

X. Ai and J. Yu (2019). Flatness-based finite-time leader-follower formation control of multiple quadrotors with external disturbances. *Aerospace Science and Technology*, 92, 20–33.

X. Wang and X. Fan (2019). Robust Formation Control for Uncertain Multiagent Systems With an Unknown Control Direction and Disturbances. *IEEE Access*, 7(106439), 1–14.

Xiao, F. and Wang, L. (2007). Consensus problems for high-dimensional multi-agent systems. *IET Control Theory and Applications*, 1(3), 830–837.

Y. Hua and X. Dong and Q Li and Z. Ren (2017). Distributed Time-Varying Formation Robust Tracking for General Linear Multiagent Systems With Parameter Uncertainties and External Disturbances. *IEEE Transactions on Cybernetics*, 47(8), 1959–1969.

Z. Zeng and X. Wang and Z. Zheng (2016). Convergence analysis using the edge Laplacian: Robust consensus of nonlinear multi-agent systems via ISS method. *International Journal of Robust and Nonlinear Control*, 26, 1051–1072.